doi:10.1246/cl.2011.1360
Published on the web November 19, 2011

Raman, UV–vis, and CD Spectroscopic Studies of Dodecameric Oxyhemocyanin from *Carcinus aestuarii*

Niels H. Andersen,[1,#] Giorgio Zoppellaro,[1,#] Luigi Bubacco,[2] Luigi Casella,[3] and K. Kristoffer Andersson*[1]
[1]*Department of Molecular Biosciences, University of Oslo, P. O. Box 1041 Blindern, NO-0316, Norway*
[2]*Department of Biology, University of Padova, 35121, Italy*
[3]*Department of General Chemistry, University of Pavia, Via Taramelli 12, 27100 Pavia, Italy*

(Received September 8, 2011; CL-110750; E-mail: k.k.andersson@imbv.uio.no)

The stable dodecameric oxy form of *Carcinus aestuarii* hemocyanin (*Cae* oxy-Hc) has been probed by resonance Raman, UV–vis, and CD spectroscopy. A clear signal emerged at 746 cm^{-1} (Raman) sensitive to isotopic exchange with $^{18}O_2$ (−40 cm^{-1}), thus confirming the presence of a μ-η^2:η^2 peroxide coordinated to the cupric centers. The optical fingerprints of *Cae* oxy-Hc show that symmetry breaking exists at the Cu(II)–O_2^{2-}–Cu(II) core and that exciton coupling effects are present in the visible region of the spectra.

Hemocyanins (Hc) are oxygen carrier and storage proteins found in molluscs and arthropods.[1] The two *phyla* differ in size of the individual subunits, ternary and quaternary protein structures, but share the same architecture for the functional oxygen binding unit. The active site contains two copper atoms ligated by six histidine (His) residues provided by protein backbone, and following interaction with molecular oxygen generates a $His_6Cu_2O_2$ core.[2] In Hc, the two copper centers are nonequivalent (hence referred to as Cu_A and Cu_B) due to minor differences in structure and accessibility of solvent as well as reactivity toward small molecules.[3] The overall symmetry of the holohedrized $His_6Cu_2O_2$ site, based on the published crystal structure of oxy-Hc from *L. polyphemus*, approaches C_{2h} symmetry, if dihedral angles of the imidazole planes are disregarded.[4] Each copper ion can be described by a ligand field geometry nearly square pyramidal, with one histidine located in axial position, two histidine and two oxygen atoms in equatorial position. The Cu–N bond lengths in oxy-Hc are 1.9–2.3 Å, with metal–metal separation of 3.6–3.7 Å (*L. polyphemus*, resolution 2.4 Å, PDB code 1OXY).[4] Such distances are consistent with those obtained experimentally by EXAFS analysis for the closely related Hc *P. interruptus*[5] and nearly identical to those obtained theoretically by DFT calculation of the $His_6Cu_2O_2$ model (Figure 1). This structural arrangement differs from that found in tyrosinases, where the symmetry of the dicopper site is closer to C_{2v}.[6] In the oxy form (oxy-Hc) dioxygen is bound as peroxide in the μ-η^2:η^2 fashion, which gives an EPR-silent ($S_T = 0$) blue Cu(II)–O_2^{2-}–Cu(II) dicopper cluster. *C. aestuarii* (*Cae*) Hc is a large protein (75 kDa subunit) where the dodecameric form represents the most stable aggregation state.[7] Calcium ions, L-lactate,[7,8] and sugar moieties give functional stability to the dodecamers against hexamers or other aggregation forms. The oxy-Hc *Cae* exhibits Bohr effect, hence providing a complicated allosteric system for binding and release of molecular dioxygen.[1] Structural details are not yet available for *Cae* Hc in either oxy and deoxy forms. However, recently the primary structure analysis of the γ-type 75 kDa (*Cae* SS2, *Cae* structural subunit 2), in combination with structure-based sequence alignments, tryptophan fluorescence, and glycosylation analyses provided important insights on its structural and functional organization.[9]

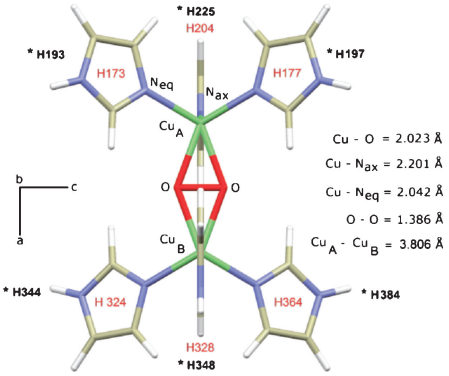

Figure 1. Theoretical model (RB3LYP/LACVP*) of the low-spin $(His_6Cu_2O_2)^{2+}$ core (dication, $S_T = 0$, gas phase) present in hemocyanins with optimized structure obtained under C_{2h} symmetry. The calculated relevant distances (Cu–N, Cu–O, O–O, and Cu–Cu) are reported on the right side of the drawing; for comparison, the histidine residues from protein backbone binding the copper metal ions as found in Hc from *L. polyphemus* are marked in red, and those thought to bind the coppers in *Cae* are marked with an (*).

The structure analysis identified conserved histidine residues that are expected to bind the copper ions (Figure 1, * labels) in similar fashion as in other Hc's of various origin. Here we report the first resonance Raman spectroscopic study of *Cae* oxy-Hc in its dodecameric state, where clear fingerprints associated to the Cu(II)–O_2^{2-}–Cu(II) dicopper site are disclosed. The work is complemented by UV–vis absorption and CD measurements that suggest, using spectra deconvolution analysis, the presence of geometric differences in coordination environment between the two copper centers. From the sequence generated *Cae* SS2, the many fluorescent tryptophans in *Cae* Hc and their proximity to the dicopper oxygen binding core (ten Trp residues located at distances 8–34 Å from His_6Cu_2)[9] make assessment of the peroxide band in oxy-Hc *Cae* by Raman spectroscopy difficult to resolve. It was in fact not possible to reveal such a signal with accuracy when experiments were performed at liquid nitrogen temperature ($T = 77$ K), due to remarkable increase in protein fluorescence being accompanied by the dominant vibrational feature of the tryptophan groups[10] (Trp, ν = ca. 760 cm^{-1}) falling near the peroxide band (Figure 2A, ν_{O-O} = ca. 747 cm^{-1}).

Furthermore, protein fluorescence increased almost exponentially upon increasing the excitation energy (e.g., changing

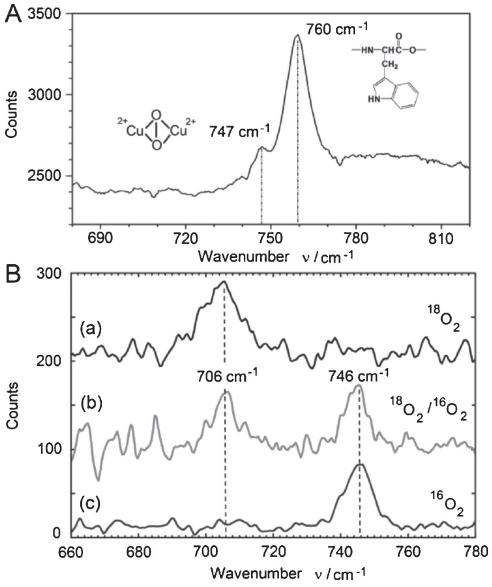

Figure 2. (A) Resonance Raman spectrum of *Cae* oxy-Hc (excitation at 532 nm) recorded at $T = 77$ K, 60 scans, 60 min, 100 mW. (B) Resonance Raman spectra of *Cae* oxy-Hc (excitation at 532 nm) recorded at $T = 293$ K with (a) $^{18}O_2$ exchange, (b) mixture (1/1, vol/vol) of $^{18}O_2/^{16}O_2$ and (c) with $^{16}O_2$, 100 scans, 100 min, 100 mW. The protein concentrations in (A) and (B) were 1.3 mM, Tris buffer (pH 7.5, 50 mM) containing $CaCl_2$ (20 mM) and sucrose (20%). The 90° scattering geometry were used, the grating employed had 3600 grooves/mm and entrance slit-width was 100 µm. The frequency scale was calibrated with 4-acetamidophenol.

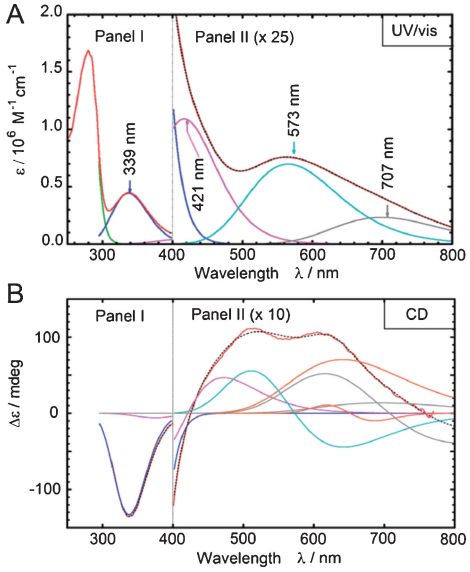

Figure 3. (A) UV–vis and (B) CD spectra of oxy-Hc *Cae* (Tris buffer, pH 7.5, 50 mM, containing $CaCl_2$ 20 mM, and sucrose 20%) showing the band-deconvolution analysis together with the total spectrum-fit (black ····· dotted).

excitation from 532 to 410 nm). Nevertheless, we found that the broad fluorescence bands at room temperature could be kept at sufficient low level allowing subtraction of their contributions from the resonance Raman signal. In addition, the presence of sucrose in the protein solution in high concentration, necessary to prevent fast protein degradation, required further careful spectral corrections. The Raman measurements performed at room temperature ($T = 293$ K) of *Cae* oxy-Hc using excitation wavelength at 532 nm gave the best results (Figure 2B, (c) spectrum) and allowed detection of a clear symmetric peroxide stretching frequency, at $746 \pm 1\ cm^{-1}$. This frequency value supports formation of a μ-η^2:η^2 type coordinated dioxygen in the $Cu_2O_2His_6$ core. Such signal was not observed when the protein was deoxygenated by gentle argon exchange combined with addition of minimum amount of sodium dithionite (2 mM, 50 mM Tris Buffer, 50 mM, pH 7.5). After deoxygenation–oxygenation cycles performed on ice ($T = 277$–280 K) and by employing a mixture of 50% vol/vol of $^{16}O_2/^{18}O_2$ gas, two peaks could be observed in the Raman spectrum (Figure 2B, (b) spectrum); one peak at $746 \pm 1\ cm^{-1}$ and the second peak at $706 \pm 1\ cm^{-1}$, having equal intensities. Those mirrored statistically occupied centers having Cu(II)–$^{18}O_2^{2-}$–Cu(II) and Cu(II)–$^{16}O_2^{2-}$–Cu(II). Upon employing pure $^{18}O_2$ gas (99.9%), the spectrum revealed a clear downshift of $40\ cm^{-1}$ in the signal (Figure 2B, (a) spectrum, $706 \pm 1\ cm^{-1}$) and demonstrated that the observed signature arises from side-on peroxide bound to the metal cluster.[11] The observed frequency in *Cae* oxy-Hc is slightly higher than that reported for oxy-Hc from *L. polyphemus* ($\nu_{O-O} = 744\ cm^{-1}$) or *C. magister* ($\nu_{O-O} = 744\ cm^{-1}$) but slightly lower than those found in *B. canaliculatum* ($\nu_{O-O} = 749\ cm^{-1}$) and *Octopus* ($\nu_{O-O} = 749\ cm^{-1}$).[11] The absorption spectrum of oxy-Hc in the UV–vis range is reported in Figure 3A. The spectrum is dominated by intense aromatic protein bands (ca. 280 nm). The charge-transfer (CT) bands associated to transitions involving the type III copper(II) exhibit much weaker absorptions, spanning in the 330–800 nm region.[11,12] Finally, the d–d Cu(II) transitions should fall at ca. 700 nm but are so weak and broad that they remain hidden within the Cu(II) CT absorption envelope occurring at nearly the same energy region.[11d] Although taken with caution, the energy range is fully consistent with that estimated by TDDFT/TDA calculation performed on the C_{2h} symmetric $(His_6Cu_2O_2)^{2+}$ model compound (Figure 4).[13] From the spectrum, band-deconvolution analysis suggests the presence of four dominant Gaussian bands in the charge-transfer region and one additional Gaussian band for the aromatic region. The sum of these components were fit to the spectrum at an energy scale with the ordinate divided by energy. Thus, transforming back to a wavelength scale with an absorption coefficient ordinate, the resulting bell curves appear asymmetric. The same procedure has been employed for the analyses of the CD spectrum. Two of the CT bands are assigned as peroxide π_σ^* and π_v^* to Cu(II) transitions (horizontal and vertical). These transitions split into four components under C_{2h} symmetry. However, disruption of the symmetry (e.g., down to C_1 as it occurs when Cu_A and Cu_B are differently coordinated) should give rise to the presence of weak and broad subbands. In addition, the Cu(II) ions in ligand fields of low symmetry, cause four d–d transitions for each copper ion to be partially allowed.[14] Such features are difficult to unveil from a UV–vis spectrum around 700 nm due to their expected broadness, and we could not detect them in the CD spectrum. The recorded CD envelope, in the low energy region, discloses a strong local symmetry breaking of the $Cu_2O_2His_6$

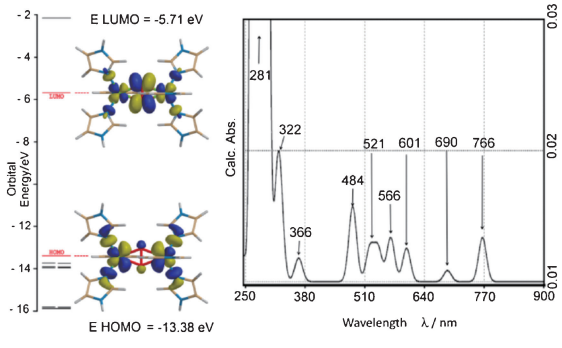

Figure 4. The UV–vis spectrum (20 nm Gaussian band-width) of the $(His_6Cu_2O_2)^{2+}$ core generated by single point (SP) energy calculation (first excited) of the optimized structure shown in Figure 1 by TDDFT/TDA (RB3LYP/LACVP*, N-states = 32) employing frozen-core approximation. The HOMO and LUMO molecular orbitals are drawn on the left side of the panel (0.032 isoVal).[16]

core (Figure 3B). The near-UV region (250–400 nm) has been analyzed thoroughly in previous work where protein interaction with small molecules binding to the copper centers has been probed.[15]

The CD spectrum analysis reveals, with two minor exceptions, that all band positions are in harmony with those derived from the UV–vis spectra (339, 421, 573, and 707 nm). Nonetheless, additional minor Cotton effect induced bands centered around 651 and 528 nm could be added to the fit. This result does not hamper the possibility that there may exist several broad subbands in this region. The first CT band near 339 nm, assigned (Cu(II) $\leftarrow \pi_\sigma^*$), exhibits pure negative CD. This is an indication that this transition cannot be explained by the exciton coupling mechanism. This interpretation agrees with the requirements of single CD band contribution at the 707 nm position. Meanwhile, the CD bands at 421 and 573 nm are characterized by Cotton effect, hence these CT transitions are likely dominated by exciton couplings.[15] In conclusion, in *Cae* oxyhemocyanin, we observed a symmetric peroxide stretching frequency at 746 cm^{-1} that showed oxygen-18 downshift of 40 cm^{-1}. The signal is typical for a μ-η^2:η^2 type coordinated dioxygen Hc $Cu_2O_2His_6$ core. The optical fingerprints of the Cu–O and Cu–N CT and d–d bands were analyzed by simultaneous curve fitting of the UV–vis and CD spectra, where contribution from exciton coupling effects were dissected indicating the symmetry breaking of the dicopper core, showing two geometrically different Cu(II) ions.

GZ thanks for financial support the FP7 Programme Marie Curie Actions Intra-European Fellowship (PIEF-GA-2009-235237), KKA the Research Council of Norway (Grant No. 177661/V30) and The Cancer Foundation of Norway, and LC the University of Pavia and CIRCMSB.

References and Notes

# Contributed equally.

1 K. E. van Holde, K. I. Miller, H. Decker, *J. Biol. Chem.* **2001**, *276*, 15563.

2 K. A. Magnus, H. Ton-That, J. E. Carpenter, *Chem. Rev.* **1994**, *94*, 727.

3 E. Borghi, P. L. Solari, M. Beltramini, L. Bubacco, P. Di Muro, B. Salvato, *Biophys. J.* **2002**, *82*, 3254.

4 B. Hazes, K. H. Kalk, W. G. J. Hol, K. A. Magnus, C. Bonaventura, J. Bonaventura, Z. Dauter, *Protein Sci.* **1993**, *2*, 597.

5 a) M. C. Feiters, *Comments Inorg. Chem.* **1990**, *11*, 131. b) A. Volbeda, M. C. Feiters, M. G. Vincent, E. Bouwman, B. Dobson, K. H. Kalk, J. Reedijk, W. G. J. Hól, *Eur. J. Biochem.* **1989**, *181*, 669.

6 E. Pidcock, H. V. Obias, M. Abe, H.-C. Liang, K. D. Karlin, E. I. Solomon, *J. Am. Chem. Soc.* **1999**, *121*, 1299.

7 S. Hirota, T. Kawahara, M. Beltramini, P. Di Muro, R. S. Magliozzo, J. Peisach, L. S. Powers, N. Tanaka, S. Nagao, L. Bubacco, *J. Biol. Chem.* **2008**, *283*, 31941.

8 a) P. Dolashka-Angelova, R. Hristova, S. Stoeva, W. Voelter, *Spectrochim. Acta, Part A* **1999**, *55*, 2927. b) S. Hirota, N. Tanaka, I. Mičetić, P. Di Muro, S. Nagao, H. Kitagishi, K. Kano, R. S. Magliozzo, J. Peisach, M. Beltramini, L. Bubacco, *J. Biol. Chem.* **2010**, *285*, 19338.

9 P. Dolashka-Angelova, A. Dolashki, S. N. Savvides, R. Hristova, J. Van Beeumen, W. Voelter, B. Devreese, U. Weser, P. Di Muro, B. Salvato, S. Stevanovic, *J. Biochem.* **2005**, *138*, 303.

10 R. C. Lord, N.-t. Yu, *J. Mol. Biol.* **1970**, *50*, 509.

11 a) T. B. Freedman, J. S. Loehr, T. M. Loehr, *J. Am. Chem. Soc.* **1976**, *98*, 2809. b) J. Ling, L. P. Nestor, R. S. Czernuszewicz, T. G. Spiro, R. Fraczkiewicz, K. D. Sharma, T. M. Loehr, J. Sanders-Loehr, *J. Am. Chem. Soc.* **1994**, *116*, 7682. c) M. J. Baldwin, D. E. Root, J. E. Pate, K. Fujisawa, N. Kitajima, E. I. Solomon, *J. Am. Chem. Soc.* **1992**, *114*, 10421. d) N. C. Eickman, R. S. Himmelwright, E. I. Solomon, *Proc. Natl. Acad. Sci. U.S.A.* **1979**, *76*, 2094.

12 K. E. Van Holde, *Biochemistry* **1967**, *6*, 93.

13 *Spartan 10, Parallel Version 1.0.1*, (Q-Chem)-Wavefunction Inc., Irvine, CA 92612, USA, **2010**.

14 W. Mori, O. Yamauchi, Y. Nakao, A. Nakahara, *Biochem. Biophys. Res. Commun.* **1975**, *66*, 725.

15 a) M. Beltramini, L. Bubacco, B. Salvato, L. Casella, M. Gullotti, S. Garofani, *Biochim. Biophys. Acta, Protein. Struct. Mol. Enzymol.* **1992**, *1120*, 24. b) S. G. Telfer, T. M. McLean, M. R. Waterland, *Dalton Trans.* **2011**, *40*, 3097. c) *Circular Dichroism: Principles and Applications*, ed. by N. Berova, K. Nakanishi, VCH Publishers, New York, **1994**. d) F. Tuczek, E. I. Solomon, *Coord. Chem. Rev.* **2001**, *219–221*, 1075.

16 Supporting Information is available electronically on the CSJ-Journal Web site, http://www.csj.jp/journals/chem-lett/index.html.

